Journal Name

ARTICLE

Mimicking the endothelial glycocalyx through supramolecular presentation of hyaluronan on patterned surfaces

Received 00th January 20xx,
Accepted 00th January 20xx

DOI: 10.1039/x0xx00000x

www.rsc.org/

Xinqing Pang,[a,b] Weiqi Li,[a,b] Eliane Landwehr,[c] Yichen Yuan,[a,b] Wen Wang,[a,b] and Helena S. Azevedo*[a,b]

The glycocalyx is the immediate pericellular matrix that surrounds many cell types, including endothelial cells (ECs), and is typically composed of glycans (glycosaminoglycans, proteoglycans, glycoproteins). The endothelial glycocalyx is rich in hyaluronic acid (HA), which plays an important role in the maintenance of the vascular integrity, but fundamental questions about the precise molecular regulation mechanisms remain unanswered. Here we investigate the contribution of HA on the regulation of the endothelial function using model surfaces. The peptidesequence GAHWQFNALTVR, previously identified by phage display with strong binding affinity for HA and named as Pep-1, was thiolated at the N-terminal to form self-assembled monolayers (SAMs) on gold (Au) substrates, and microcontact printing (μCP) was used to develop patterned surfaces for the controlled spatial presentation of HA. Acetylated Pep-1 and a scrambled sequence of Pep-1 were used as controls. SAMs and HA-coated surfaces were characterized by X-ray photoelectron spectroscopy (XPS), contact angle measurements and quartz crystal microbalance with dissipation (QCM-D) monitoring, which confirmed the binding and presence of thiolated peptides onto the Au surfaces and the deposition of HA. Fluorescence microscopy showed the localization of fluorescently labelled HA only on areas printed with Pep-1 SAMs. Cell culture studies demonstrated that low molecular weight HA improved adhesion of human umbilical vein endothelial cells (HUVECs) to the substrate and also stimulated their migration. This research provides insights on the use of SAMs for the controlled presentation of HA with defined size in cultures of HUVECs to study their functions.

1. Introduction

Hyaluronic acid (HA), or hyaluronan, is a linear polysaccharide that consists of repeating disaccharide units of N-acetylglucosamine and glucuronic acid.[1] Despite its simple chemical structure, HA exhibits remarkable wide-ranging and often opposing biological functions and these activities seem to be related with HA molecular size.[2] High molecular weight HA is known to be space-filling, immunosuppressive and anti-angiogenic. Molecules up to 20 kDa in size participate in the processes of ovulation and embryogenesis, wound healing, while smaller HA oligosaccharides are known to be inflammatory, immune-stimulatory and pro-angiogenic. HA is found in almost all living organisms, being degraded and resynthesized on a daily basis in the human body.[3] HA usually exists in the extracellular matrix (ECM), which provides cells with a physical and chemical microenvironment that determines their proliferation, migration or differentiation.[4] The vascular endothelial glycocalyx, a brush-like layer located in the luminal surface of the vascular endothelium, is also rich in HA. Current studies suggest that the glycocalyx is a crucial component of many vascular activities, such as blood tissue exchange, inflammatory response, tissue homeostasis, fibrinolysis, coagulation, vascular regulation, vasodilation of various tissues, and angiogenesis.[5-11] HA is the only non-sulfated glycosaminoglycan (GAG) that binds to cell surface receptor CD44 and the multitude of biological activities depends on its length. As a highly hydrophilic molecule, HA contributes to tissue hydrodynamics and the transport of water, and plays an important role in cell proliferation, migration and maintaining vascular integrity.[12]

To dissect key features of the ECM, researchers have developed synthetic platforms with defined chemistry that act as model surfaces for studying specific ECM-cell interactions.

Self-assembled monolayers (SAMs), the spontaneous assembly of organosulfur compounds on metal surfaces, have been widely applied to prepare biocompatible substrates with defined chemical composition for biomedical research, including wetting, protein adsorption and cell adhesion studies.[13-15] In particular, gold (Au) has been the standard surface for creating SAMs because it is not toxic to cells and has high binding affinity to thiols along with its inert characteristics.[16] Molecules used in SAMs typically consist of three parts: a head group (a thiol group), an alkyl chain and a tail functional group (-CH_3, -COOH, -PO_3^{2-}, -OH).[17]

[a] School of Engineering and Materials Science, Queen Mary University of London, London E1 4NS, UK
[b] Institute of Bioengineering, Queen Mary University of London, London E1 4NS, UK
[c] Department of Chemistry, University of Konstanz, Konstanz 78464, Germany

†Electronic Supplementary Information (ESI) available. See DOI: 10.1039/x0xx00000x

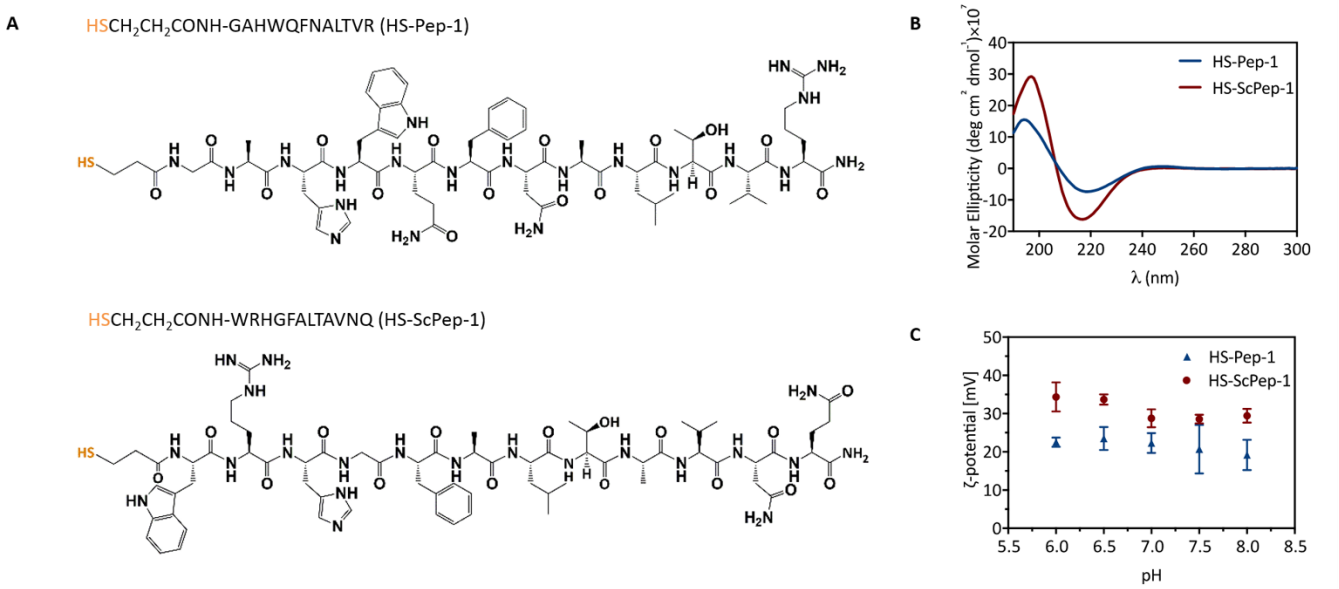

Fig. 1 Thiol-containing peptides used to create SAMs on Au surfaces and their characterization. (A) Chemical structure of thiolated HA-binding peptide (HS-Pep-1) and thiolated scrambled Pep-1 (HS-ScPep1). (B) Circular dichroism (CD) spectra of the peptides at pH 7 and 0.1 mg/mL. (C) Zeta potential of the peptides at different pH values within the range 6 to 8.

The mechanism of SAM formation includes two steps: the rapid and strong chemisorption between head groups and Au substrates, and the subsequent slow reassembly due to the interaction between the alkyl chains (van der Waals' forces).[18-20] The structure and quality of SAMs formed on Au substrates are affected by factors such as surface roughness, concentration and purity of self-assembled molecules, immersion time, solvents and temperature.[21-24] The formation, composition, and structure of SAMs has been characterized by complementary characterization techniques, such as X-ray photoelectron spectroscopy (XPS)[25], quartz crystal microbalance with dissipation (QCM-D)[26, 27] and contact angle.[28-31]

Functional peptides attached to Au surfaces, forming well-arranged and reproducible SAMs, have been used in many biomedical studies.[32] For example, the work by Mrksich on using SAMs as ECM models has largely contributed to elucidate the role of peptide and protein ligands in cell–matrix interactions. In particular, SAMs presenting the Arg-Gly-Asp (RGD) peptide with different densities and spacing were used to investigate the adhesion and spreading of different cell types.[33]However, the application of peptides binding to specific components of the ECM has not yet been exploited.

Mummert et al. identified a HA-binding peptide (GAHWQFNALTVR) through phage display technology, named as Pep-1, which presented specific binding to soluble, immobilized, and cell-associated forms of HA.[34] The ability of Pep-1 to bind to both HA-coated substrate and HA molecules expressed on the surfaces of endothelial cells was also demonstrated.[34]

In this study, we have modified Pep-1 with thiol functionality (Fig. 1A) to form Pep-1 SAMs on Au which would result in surfaces displaying multiple peptide sequences with binding affinity for HA (Fig. 2). In addition, using microcontact printing (μCP), patterns of Pep-1 SAMs could be created on Au surfaces for the spatial localization of HA. μCP consists in transferring an ink solution from a patterned elastomeric mould, or stamp, to a substrate by contact with its surface.[35, 36] The combination of μCP and SAMs is advantageous for obtaining good control over the surface chemistry and minimizing defects due to the molecular self-organization.[35]

We hypothesized that the supramolecular (non-covalent) immobilization of HA with defined sizes on surfaces could be used to probe how endothelial cells sense and respond to distinct HA sizes and would provide insights on the effect of HA on important cellular functions of the endothelium in health and diseases.

2. Materials and methods

Protection of 3-mercaptopropionic acid

To ensure coupling of the acid group of 3-mercaptopropionic acid with free amino in the peptide N-terminal, 3-(((4-methoxyphenyl)diphenylmethyl)thio)propanoic acid was synthesized. N, N-Diisopropylethylamine (DIPEA, Sigma) and 3-mercaptopropionic acid were added dropwise into a stirring solution of 4-methoxytriphenylmethyl chloride (MMT, Sigma), in 1:1 dichloromethane (DCM, Sigma) / dimethylformamide (DMF, Sigma). The reaction mixture was concentrated by rotary evaporation, suspended in water and then washed with diethyl ether. The organic layer was washed with brine, dried over magnesium sulfate (Thermo Scientific) and concentrated to oil by rotary evaporation. The oil was dried under high vacuum until leaving a white powder. The chemical structure of the obtained product was confirmed using nuclear magnetic resonance (NMR, ESI, Fig. S1).

Peptide synthesis and purification

Pep-1 (GAHWQFNALTVR) and a scrambled sequence (ScPep-1, WRHGFALTAVNQ)[37] were synthesized in an automated microwave peptide synthesizer (Liberty Blue, CEM, UK) on a 4-methylbenzhydrylamine (MBHA) rink amide resin (bead size: 100–200 mesh, Novabiochem) following the standard 9-fluorenylmethoxycarbonyl (Fmoc) solid phase peptide synthesis protocol. DCM was used to swell the resin and 20% (v/v) piperidine (Sigma) in DMF was used as deprotection solution. The coupling was performed using 4 mol equivalents of Fmoc-amino acid (Novabiochem), 1-hydroxybenzotriazole hydrate (HOBt) and N,N'-diisopropylcarbodiimide (DIC). The 3-(((4-methoxyphenyl)diphenylmethyl)thio)propanoic acid tail was manually coupled on the N-terminal of the peptide under the same condition as the Fmoc-amino acids. For the acetylated Pep-1 (Ac-Pep-1), the N-terminal was capped with acetyl group by incubating the peptide-bound resin with 10% (v/v) acetic anhydride (Sigma) in DMF under shaking for 10 min. The coupling of the thiol tail or acetylation was confirmed by the Kaiser test kit (Sigma), where negative results (no free amine groups) indicated successful coupling and capping. The cleavage of final peptide from the resin and the removal of the protecting groups was performed by shaking the resin with bound peptide with a mixture solution containing trifluoroacetic acid (TFA, Sigma)/ thioanisole (Sigma)/ 1,2-Ethanedithiol (EDT, Sigma)/anisole(Sigma) (90%/5%/2.5%/2.5%) for thiol-containing peptides and TFA/ triisopropylsilane (TIS, Sigma)/water (95%/2.5%/2.5%) for the Ac-Pep-1 at room temperature for 3 hours. Peptides were concentrated using rotary evaporator and subsequently precipitated in cold diethyl ether. The resulting suspension was centrifuged (Heraeus Multifuge X1, Thermo Scientific) at 4100 rpm for 20 minutes and the powder collected for freeze-drying. The mass of crude peptides was confirmed by electro-spray ionization mass spectrometry (ESI-MS, Agilent) and their purity was examined in an Alliance high-performance liquid chromatography (HPLC) system (Waters) coupled with an analytical reverse-phase C18 column (XBridge, 130 Å, 3.5 µm 4.6 x 150 mm, Waters). The peptide bond was used for detection through a UV/Vis detector (2489, Waters) set at 220 nm and Empower software®. Peptide solutions (1 mg/mL, 100 µL) were injected into the column and eluted at 1 mL/min using a water/acetonitrile (ACN, Sigma) (0.1% TFA) gradient. An AutoPurification preparative scale HPLC system (Waters 2545 Binary Gradient HPLC system, Waters) containing reverse-phase C18 column (X-bridge, 130 Å, 5 µm, 30×150 mm, Waters) was used to purify the peptides. Peptides were eluted at 20 mL/min using a gradient of water/ACN containing 0.1% TFA. Fractions were collected based on the mass detection performed by SQ detector 2 (Waters) and the data were processed in MassLynx® software. After the purification process, the solvent was removed by rotary evaporation followed by freeze-drying. Finally, the purity of the peptides was confirmed by ESI-MS and analytical HPLC, as described above.

Peptide characterization

Zeta potential. To investigate the overall charge of HS-Pep-1 and HS-ScPep-1 at different pHs within the range 6 to 8, the ζ-potential of peptide aqueous solutions was measured using Nano-ZS Zetasizer (Malvern Instruments). Briefly, peptides were dissolved in ultrapure water (0.1 mM) and the pH was adjusted to 6, 6.5, 7, 7.5 and 8 by adding 0.1 M HCl or 0.1 M NaOH. Cuvettes containing gold electrodes (DTS1070, Malvern Panalytical) were used to load the peptide samples, and the ζ-potential was recorded at 25 °C.

Circular dichroism (CD) spectroscopy. The secondary structure of HS-Pep-1 and HS-ScPep-1 was characterized by CD. Peptides were dissolved in ultrapure water (0.1 mg/mL) and the pH was adjusted to 7. The 1 mm path length quartz cuvette was used to load peptide aqueous solutions, and the CD spectra were recorded at 25 °C from 190 to 300 nm performed in a PiStar-180 spectrometer (Applied Photophysics). Ultrapure water was measured to obtain a background spectrum which was subtracted from the peptide sample spectra. Each represented spectrum is an average of 3 spectra. The molar ellipticity $[\theta]$ at wavelength λ was calculated using the following equation (1):

$$[\theta] = \frac{100 \times \theta}{c \times d} \quad (1)$$

θ is the observed ellipticity in mdeg, c is the concentration of peptide solution in molar and d is the cuvette path length in cm.

Preparation of peptide SAMs and HA deposition

The gold-coated slides used in this study were either purchased from Dynasil (5 nm chrome followed by 100 nm gold) for SAMs characterization experiments or coated with 5 nm chrome followed by 20 nm gold through evaporation in the School of Physics & Astronomy at Queen Mary University of London to perform microscopy in the cell culture assays. The HA used in all experiments was purchased from Lifecore Biomedical, Inc. (Chaska). Briefly, slides were submerged in an ethanolic solution (ethanol/water in a 9:1 ratio) containing 0.1 mM peptide (HS-

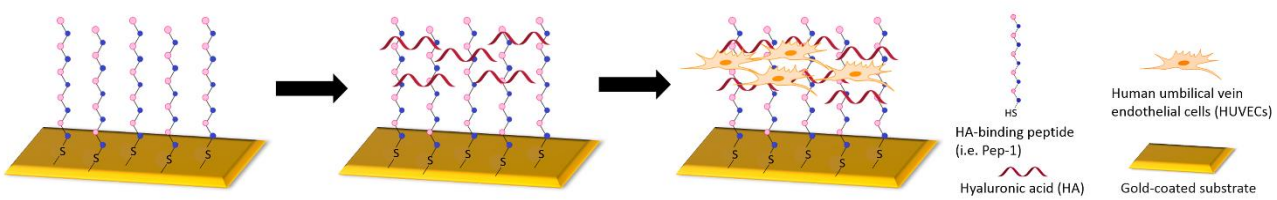

Fig. 2 Schematic representation of the fabrication process to obtain HA coated surfaces for cell culture using self-assembled monolayers of HA-binding peptide.

Pep-1 or HS-ScPep-1) and incubated at room temperature overnight (Fig. 2). The slides were rinsed with ethanol, dried under N_2 and then incubated with a 0.5 mg/mL aqueous solution of unmodified HA (molar mass of either 5 kDa, 60 kDa, or 700 kDa) for at least 24 hours at room temperature (Fig. 2). The HA-coated surfaces were rinsed with ultrapure water to remove weakly bound molecules, dried under N_2 and characterized or used in further studies.

Fluorescein-hyaluronic acid (HA)

HA was labelled with fluoresceinamine following the procedures previously described.[38, 39] Briefly, 40 mL aqueous solution of 0.25% (w/v) unmodified 700 kDa HA was mixed with 40 mL DMF containing 10 mg of fluoresceinamine (Sigma). 200 mg of N-hydroxysuccinimide (NHS, Sigma) were added to the mixture and the pH adjusted to 4.75 using 0.1 M HCl. Then, 100 mg of N-(3-dimethylaminopropyl)-N′-ethylcarbodiimide hydrochloride (EDC, Sigma) were added and the pH maintained at 4.75. After 12 h, the solution was dialyzed against 100 mM NaCl using dialysis tubing (5000 Da MWCO, Sigma) for 2 days, followed by another 2 days dialysis against ultrapure water and then freeze-dried.

Preparation of PDMS stamps and micro-contact printing (μCP)

PDMS stamps were prepared following the procedure described by Qin *et al*.[36] Briefly, Sylgard 184 silicone elastomer base and the curing agent (Dow corning), mixed in a mass ratio of 10:1, were placed in a vacuum-connected dessicator. The degassed liquid mixture was poured onto the patterned template and then placed in an oven overnight to achieve a cured PDMS stamp. The micropatterns of the PDMS stamps were imaged by scanning electron microscopy (SEM, Inspect F) using 5.0 kV beam after coated with a gold layer.

HS-Pep-1 and HS-ScPep-1 were dissolved in ethanol (1.5 mM), swabbed onto the patterned side of PDMS stamp using a cotton Q-tip and then dried under a stream of nitrogen. The loaded stamp was brought into contact with gold surface for 10 seconds. Patterned gold slides were then incubated with a 0.5 mg/mL aqueous solution of fluorescein HA (700 kDa) overnight at room temperature. Bare Au incubated with 700 kDa fluorescein-HA solution (0.5 mg/mL) was used as a control. Samples were rinsed with ultrapure water then dried under N_2. Images were then acquired using the Leica DMi8 Epifluorescence microscope (Leica) at 10× and 20× magnification.

Characterization of peptide SAMs and HA-coated surfaces

Contact angle. The contact angle of the bare Au surface, Pep-1 and ScPep-1 SAMs and coated with HA, was measured by the Sessile drop technique using a Drop Shape Analyser (Model DSA100, Krüss). 2 μL of ultrapure water was dropped onto the surface and the contact angle was measured. Bare Au immersed in 60 kDa HA aqueous solution (0.5 mg/mL) was used as control. The contact angle of each surface (>8 gold substrates) was measured in 3-5 different locations and the average was calculated.

Quartz crystal microbalance with dissipation (QCM-D). SAM formation and HA deposition was monitored by QCM-D (QS100, QSense). Before use, the gold-coated AT-cut quartz crystal (QSense) was cleaned with base piranha (30% ammonium hydroxide (Sigma)/30% H_2O_2 (Sigma)/water in a 1:1:3 ratio) at 60 °C, rinsed with ultrapure water and then dried under N_2. Cleaned crystal was then UV-Ozone treated (UVOCS T10X10 OES/E, Ultraviolet Ozone Cleaning Systems) for 20 minutes. For all experiments, baseline, deposition and washings were acquired at 37 °C in 150 mM sodium chloride (NaCl). Immediately after the baseline frequency of the crystal became stable, a solution of HS-Pep-1, Ac-Pep-1 or HS-ScPep-1 (0.1 mM in 150 mM NaCl) was injected into the crystal chamber for binding. The system was rinsed with NaCl to remove loosely bound molecules. A solution of 60 kDa HA (0.5 mg/mL in 150 mM NaCl) was then injected into the crystal chamber for binding. Again, once a stable frequency was acquired, the system was washed with NaCl solution to remove weakly associated HA molecules. The frequency (Δf) and dissipation (ΔD) changes were monitored in real time, and the results are shown for 34.7 MHz resonance. Mass changes (Δmass) were calculated using Voigt model by software QTools.

X-ray photoelectron spectroscopy (XPS). XPS analyses were performed on a Thermo Scientific™ XPS system. The analysis point area was 100 μm × 100 μm. Analyzer pass energy for survey spectra was 200.0 eV. The elemental spectra was acquired with an analyser pass energy of 50.0 eV. The spectra of Au4f, C1s, N1s, O1s, S2p and survey were analysed by software Advantage. The S peaks were fit using two S2p doublets with 2:1 area ratios and splittings of 1.2 eV. Binding energies were calibrated by setting the Au4f7/2 at 84.0 eV. Two replicates per group were measured and averaged.

Cell culture

Human umbilical vein endothelial cells (HUVECs, Lonza) were cultured in medium 199 (Invitrogen) supplemented with 10% foetal bovine serum (FBS), 1 ng/ml β-endothelial cell growth factor, 3 μg/ml bovine neural extract, 1.25 μg/ml thymidine, 10 U/ml heparin, 100 U/ml penicillin and 100 μg/ml streptomycin. All supplements were purchased from Sigma. Cells were cultured in a 5% CO_2 incubator at 37 °C. Culture medium was exchanged every 2 days. Solutions of HS-Pep-1 (0.1 mM), HS-ScPep-1 (0.1 mM) and HA (0.1 mg/mL) used in the cell culture were sterilized under UV light for 30 min before SAMs preparation.

Cell adhesion and migration assay

Gold-coated microscope slides (cut into ~0.5” ×0.5” pieces) were placed in a 12 well plate and SAMs were formed as described above. HUVECs were seeded at a density of 5×10^4 cells/well. To investigate the extent of cell adhesion, the spreading area of cells was measured at 30, 60 and 90 mins immediately after seeding. Images were obtained at 10× magnification using optical microscope (DFC420 C, Leica). Only attached cells were considered for calculation of the cell area (Fig. 5, A3, green arrow). Cells maintaining a round shape (not

adhered to the substrate) were not considered (Fig. 5, A3, yellow arrow). Cell areas were calculated using image J. To track cell movement, time-lapse images were obtained every 10 min using Lumascope 720 (Etaluma) at 37 ℃ and 5% CO_2. The cell trajectory and velocity were analysed using Image J.

Cell viability assay

8 well sticky-Slides (ibidi) were assembled on Dynasil gold coated slides (1" ×3") and SAMs were formed as described above. The metabolic activity of HUVECs over 24 and 48 h incubation periods was assessed using the AlamarBlue™ cell viability reagent (ThermoFisher). AlamarBlue™ (10% volume of the well) was added to cell culture medium and then incubated at 37 ℃ and 5% CO_2 for 4 hours protected from direct light. After incubation, the absorbance values were read at 570 nm and 600 nm on a BMG Labtech microplate reader. The percent reduction was calculated following the manufacturer's instructions.

Data analysis and statistics

All data values are expressed as mean ± standard deviation (SD). Statistical analysis was performed using GraphPad Prism 7.00 software. Statistical significance was evaluated using unpaired t-test for zeta potential data. Statistical differences of other experiments were determined using one-way analysis of variance (ANOVA) with a Tukey's honest significant difference (HSD) post-hoc test. Statistical significant difference between groups was accepted at $P < 0.05$.

3. Results and discussion

Peptide SAMs on gold have been used to create defined surfaces for identifying substrates able to support cell adhesion[40] and proliferation[41] or prevent protein adsorption (non-fouling surfaces).[32, 42] Peptides can be attached to Au surfaces using the thiol functionality of cysteine, either at the N- or C-terminus.[32, 43, 44] However, using cysteine to anchor the peptide onto the Au surface does not allow obtaining well-packed and dense monolayers due to the steric hindrance caused by the N-terminal. To circunvent this problem, researchers have conjugated peptides with alkanethiols at both termini[40, 42, 45] or by incorporating a linker sequence of four proline residues linked to the terminal cysteine to confer rigidity and ensure closely packed monolayers.[32] Here, we synthesized peptides with a free thiol group at the N-terminus (Fig. 1A) using a bifunctional molecule (3-mercaptopropionic acid). The thiol functionality was protected first with MMT group (ESI, Fig. S1) to allow coulpling of the carboxylic acid of the mercapto acid to the free amine of the peptide N-terminus. We expect that this peptide configuration will promote the formation of well-ordered SAMs.

Peptides characterization

To gain insights on the secondary structure adopted by the peptides used to form SAMs, CD spectroscopy was conducted on the peptides in solution. The CD spectrum of HS-Pep-1 showed a positive maximum at 194 nm and the negative maximum appeared at 218 nm (Fig. 1B). For HS-ScPep-1, the positive maximum was in 197 nm and the negative maximum at 217 nm. These are characterisitic signatures of a β-sheet structure.[46] A β-sheet structure suggest the ability for peptide interchain interactions through hydrogen bonds. The zeta potential of HS-Pep-1 and HS-ScPep-1 showed a positive charge for both peptides, as expected. There are two amino acids with ionizable side chains, the amine groups of arginine (R, pKa>10) and the imidazolium group of histidine (H, pKa=6.1). The amine group of R is protonated in the pH range studied while H carries a positive charge at pH<6. HS-ScPep-1 had higher (significant different in the t-test analysis) zeta potential compared to HS-Pep-1 in the pH range 6-8 (Fig. 1C) despite having exactly the same amino acid composition. Both peptides are higly hydrophobic, containing only 25% hydrophilic amino acids. However, their position in the peptide backbone is not the same leading to a different distribution of hydrophobic and hydrophilic amino acids and resulting in different interactions among peptide molecules and with the solvent. CD data indicates a more pronounced β-sheet signal for the HS-ScPep-1 which may lead to the formation of more stable aggregates with higher surface charge.

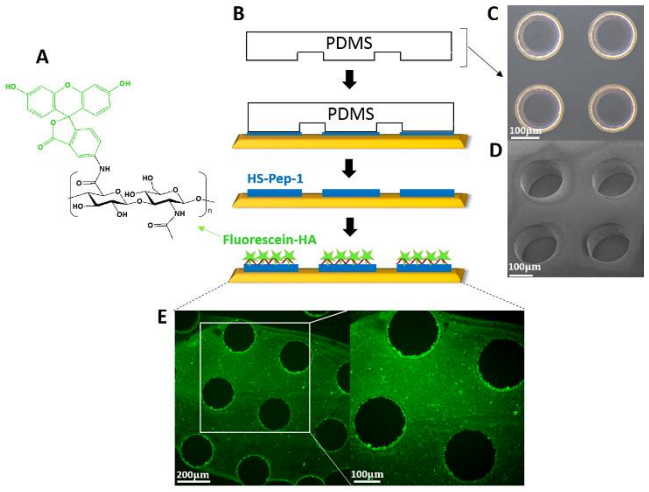

Fig. 3 Schematic illustration showing the creation of HA patterns by μCP. (A) Chemical structure of fluorescein-HA. (B) Flow diagram of μCP. HS-Pep-1 was loaded on gold surface by PDMS stamp, then substrate was immersed in fluorescein-HA solution allowing binding to attached Pep-1. (C) Bright filed microscopy images of patterned PDMS mold. (D) SEM images of patterned PDMS mold. (E) Fluorescence images showing the localization of fluorescein-HA (green) on HS-Pep-1 printed areas.

Patterning HA on micro-contact printed Pep-1 SAMs

μCP technique was utilized to demonstrate the ability of using Pep-1 SAM to create HA patterns on Au surfaces (Fig. 3). PDMS molds patterned with round holes and 200 μm diameter were used to print HS-Pep-1 on Au substrate. SEM images confirmed the hollow morphology and dimension of the patterns on the PDMS mould (Fig. 3D). Using HA labelled with fluorescein (green dye) and through fluorescence microscopy, HA was shown to be localized only on the Pep-1 printed areas (Fig. 3E). No fluorescent patterns were observed on either bare Au or ScPep-1 SAM after incubation with fluorecein-HA (ESI, Fig. S5).

performed, the quartz crystal disk (QCM-D sensor) oscillates at

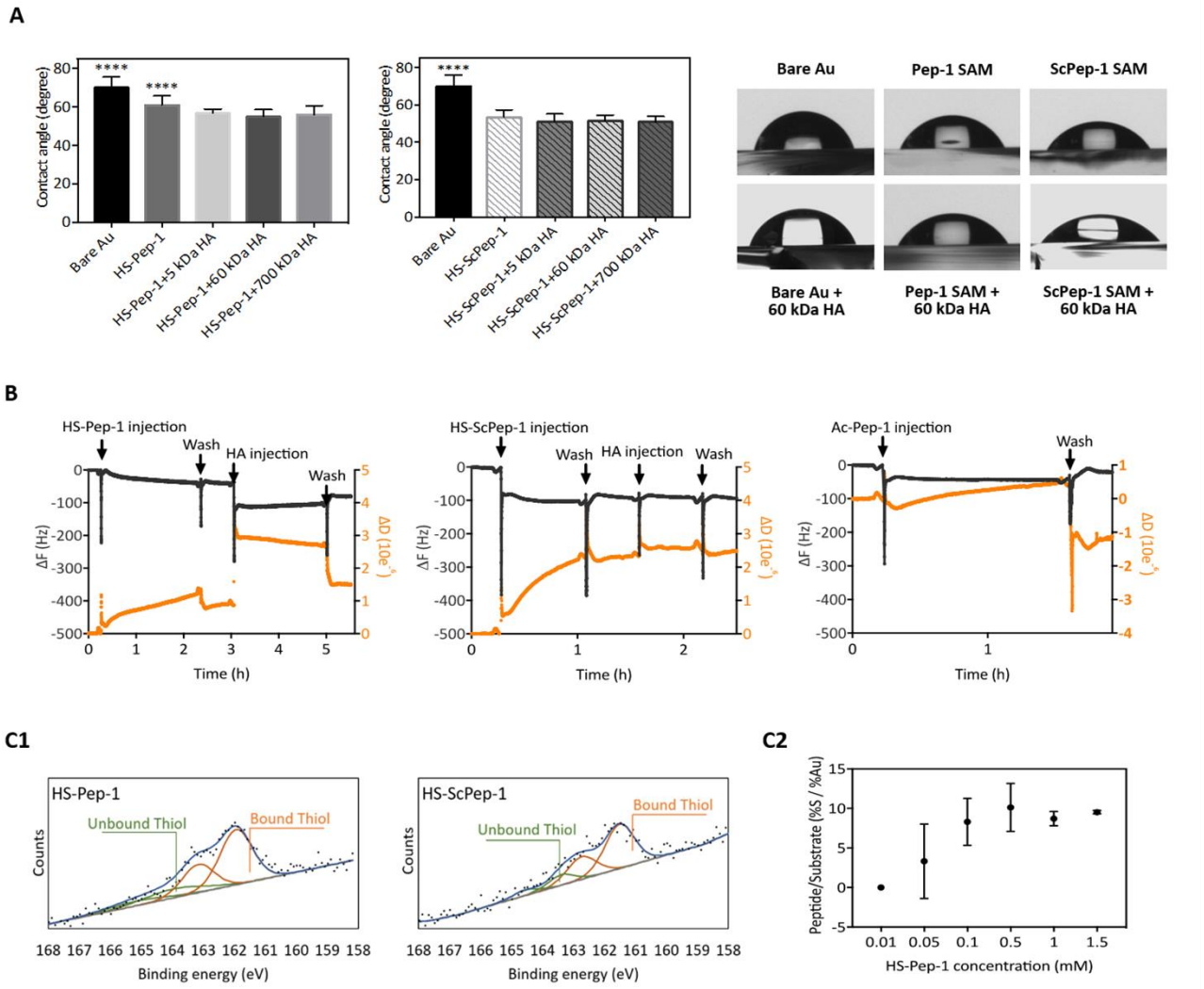

Fig. 4 Characterization of peptide SAMs formed on Au surfaces. (A) Contact angles of gold surfaces without and with peptide SAMs and after deposition of HA with different molecular weights (left: Pep-1 SAM, right: ScPep-1 SAM). (B) QCM-D monitoring of frequency changes (Δf, black) and dissipation changes (ΔD, orange) on the formation of Pep-1 and ScPep-1 SAMs followed by addition of 60 kDa HA injection and adsorption of Ac-Pep-1. (C1) XPS S2p spectra of Pep-1 (left) and ScPep-1 (right) SAMs on gold surfaces. The S peaks were fit using two S2p doublets with 2:1 area ratios and splittings of 1.2 eV. The position of the S2p3/2 peaks assigned to bound thiolate and unbound thiol are shown in orange and green, respectively. (C2) HS-Pep-1 binding isotherm on Au shown as a ratio of sulfur atomic percent to Au atomic percent (%S/%Au) for different concentrations of HS-Pep-1.

SAMs characterization

To characterize changes in hydrophilicity of the Au surfaces after modification, water contact angle was measured and compared to bare Au surface. The water contact angle on bare gold was 70.00 ± 5.59 degree showing a highly hydrophobic surface and that on Pep-1 SAMs was 60.92 ± 4.90 degree. After HA deposition, substrates became more hydrophilic compared to the bare gold and with immobilized Pep-1, suggesting the presence of HA on the surface. Surface coated with 60 kDa HA had contact angle of 54.86 ± 3.65 degree (Fig. 4A). ScPep-1 SAMs (53.35 ± 4.06 degree) showed to be more hydrophilic than the oned formed by Pep-1 and there were no significant differences between the ScPep-1 SAM and HA-coated on ScPep-1-Au surfaces. The formation of SAMs and HA deposition were followed *in situ* by QCM-D. When an alternating potential is its resonance frequency. A decrease in frequency was observed upon the addition of HS-Pep-1 and remained constant upon washing. A further decrease in frequency was observed after injection of HA (Fig. 4B). This decrease in frequency, combined with the increase in dissipation, indicates the binding of HS-Pep-1 and HA deposition on the surface of the Au crystal. When the thiol functionality was removed from Pep-1 sequence (Ac-Pep-1) the binding of the peptide was diminished and removed after washing, highliting the need for the thiol group to form stable bond with Au. The binding of HS-ScPep-1 to the Au crystal was confirmed, but when HA was injected on ScPep-1 coated crystal, there was no significant frequency shifts, indicating that HA did not bind to ScPep-1 SAMs. These results confirm that the binding affinity of Pep-1 to HA is sequence-dependent, and scrambling this sequence (ScPep-1) results in the loss of HA binding affinity. The resonance frequency changes upon mass

deposition on the crystal surface and the viscoelastic properties can be analysed using the Voigt model.[47] Mass changes compared to the base line (after washing) further demonstrated the strong affinity of Pep-1 binding to HA, the deposition mass of which increased sharply after HA injection (ESI, Fig. S6). The bond formation between S and Au was confirmed by monitoring the S2p3/2 binding energy which was obtained by XPS.[48-50] The S2p spectrum of HS-Pep-1 modified gold surface showed two peaks at 161.9 eV and 163.1 eV, assigned to bound S atoms (S2p3/2 and S2p1/2), and a peak at 163.9 eV corresponding to unbound thiols (Fig. 4, C1). The position of S2p3/2 peak for ScPep-1 modified gold surface was at 161.5 eV for bound thiolate and 163.4 eV for unboud thiol. The signal of unbound thiol on ScPep-1 SAMs was smaller than the signal for Pep-1 SAMs. Different concentrations of HS-Pep-1 (0.01 mM - 1.5 mM) were tested to investigate the coverage of the gold surfaces and density of SAMs (Fig. 4, C2; ESI, Table S4). When 0.01 mM of HS-Pep-1 was used, the sulfur composition was very low (%S/%Au ~0%). However, the sulfur composition increased with increasing peptide concentrations, 8.27 ± 2.96 % for 0.1 mM HS-Pep-1 and 9.24 ± 3.04 % for 0.5 mM HS-Pep-1, with decrease in the gold signal, indicating that SAMs were more densely packed. For higher concentration (1 mM and 1.5 mM) of HS-Pep-1, no significant changes in sulfur composition was observed, suggesting saturation of the surface from 0.5 mM HS-Pep-1. XPS was also used to confirm the binding of sulfur was responsible for the formation of SAMs on the gold surface. There was no sulfur element detected for bare Au in the XPS survey (ESI, Fig. S8). Comparison of the theoretical elemental composition of the peptides with the elemental percent composition of the peptide SAMs formed on the surface obtained by XPS (ESI, Fig.

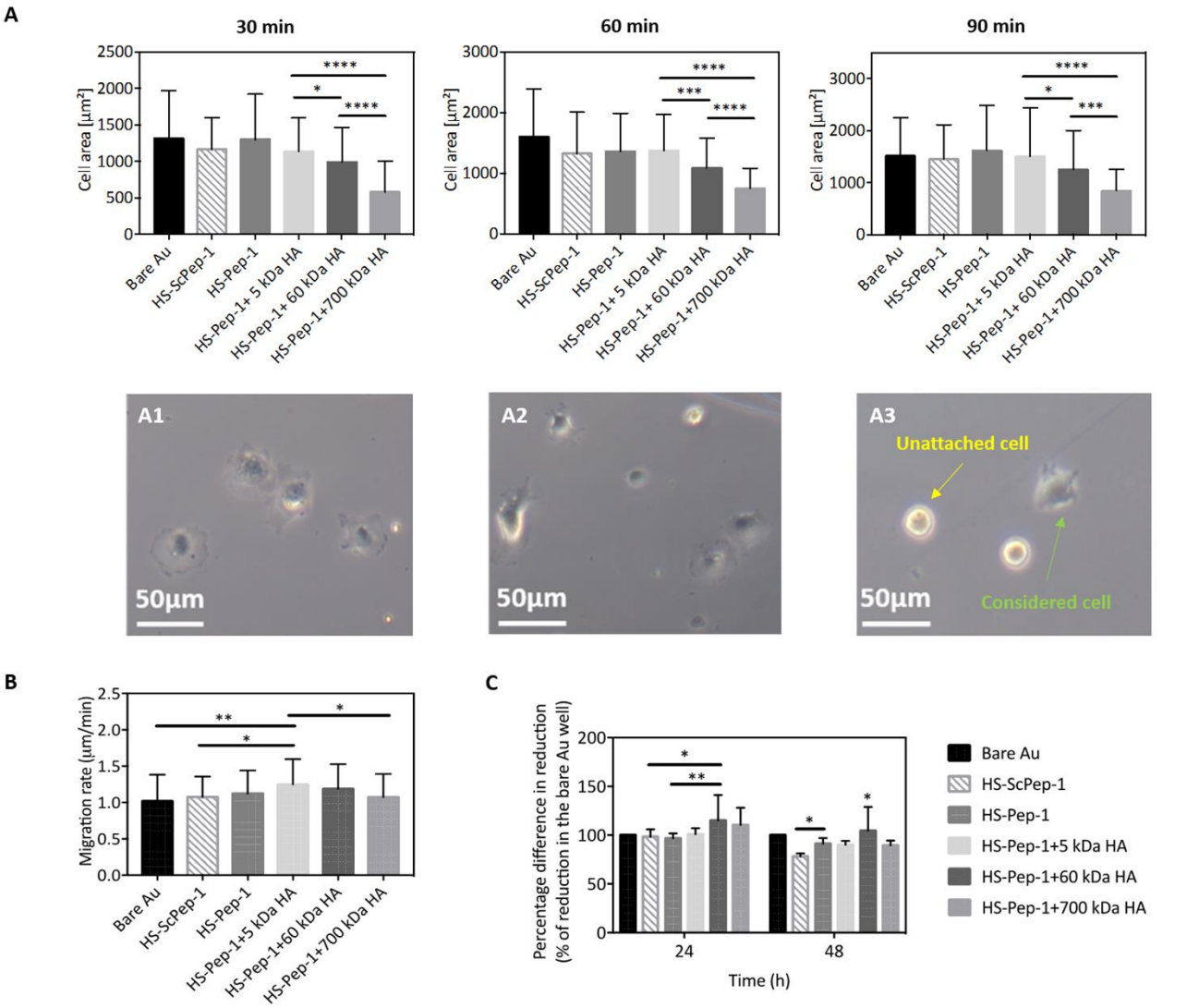

Fig. 5 (A) Spreading of HUVECs during different time periods when cultured on Pep-1-HA and HS-ScPep-1 SAMs coated with HA of different molecular weights. (A1-A3: cell spreading morphology seeded on Pep-1 SAM coated with 5, 60 and 700 kDa HA, respectively, at 60 min post-seeding. Green arrow pointing cells considered for the calculation of cell area and yellow arrow pointing cells not considered for the calculation. (B) Migration and (C) viability of HUVECs cultured on prepared surfaces.

S7) show a good correlation, further indicating the successful formation of the peptide SAMs on the Au surface.

Taken toghether, the results from QCM-D analysis and XPS characterization showed the attachment of HS-Pep-1 on bare Au through the bond between sulfur and Au. Moreover, the HA binding affinity of Pep-1 was confirmed by frequency and dissipation shifts, and the deposition of HA led to more hydrophilic surfaces.

Cell culture

The effect of HA length on culture of endothelial cells has been investigated in several studies,[51, 52] but mainly using HA in solution (added to the culture medium). Covalent immobilization of HA on solid surfaces[53, 54] has also been investigated, but the methods used require chemical modification of HA. Using the Pep-1 SAM described in the previous sections, we have studied the effect of HA molecular weight on HUVECs, where HA is presented at surfaces in its native form without covalent immobization. Through *in vitro* cell spreading experiments, low molecular weight HA (5 kDa and 60 kDa HA) was shown to stimulate cell spreading with higher cell surface areas (Fig. 5A). Cells cultured on substrates without HA (bare Au, Pep-1 and ScPep-1 SAMs) showed an advantage on spreading in the first 30 min, but this advantage gradually disappeared after 60 min of culture. 700 kDa HA slowed down the attachment of cells, with less attached cells observed at all time points, suggesting a suppresion of cell adhesion and a significant reduction of cell surface areas. For example, after cultured for 60 min, the area of cells seeded on 5 kDa HA-modifiled surfaces was 1375.72 ± 597.13 μm^2, that of 60 kDa HA-modifiled surfaces was 1091.05 ± 492.69 μm^2 and that of 700 kDa HA-modifiled surfaces significantly dropped to 751.24 ± 336.00 μm^2 (Fig. 5, A1-A3). Low molecular weight HA (5 kDa) also showed a noticeable enhancement on cell migration (Fig. 5B) with the highest migration rate at 1.25 ± 0.35 μm/min. However, cells cultured on 700 kDa HA-modified surfaces had a slow migration rate at 1.07 ± 0.32 μm/min, with only cells on bare Au having a slower rate.

These results were consistent with the literature reporting that low molecular weight HA can stimulate cell motility while high molecular weight HA inhibits.[53] In the cell viability assay, cells seeded on bare Au were used as control cells, and the percentage difference between treated (seeded on peptide SAMs with and without HA) and control cells was calculated (Fig. 5C). Cells seeded on Pep-1 SAM surfaces with 60 kDa HA showed the highest viability, with115.12 ± 26.00 % at 24 hours and 104.63 ± 24.30 % at 48 hours compared to control cells.

Conclusions

In summary, we describe the development of self-assembled monolayers on gold using a HA-binding peptide (Pep-1) as a platform to mimic the function of the endothelial glycocalyx. For that, Pep-1 bearing an N-terminal thiol group was successfully synthesized. Water contact angle measurement indicated that surfaces modified using HS-Pep-1 and HA were more hydrophilic. QCM-D monitoring further demonstrated the strong affinity of Pep-1 to bind HA when immobilized on a solid surface. XPS showed that most of the sulfur atoms on gold surface were bound thiolate species for both Pep-1 and ScPep-1 SAMs. μCP enabled spatial control over HA localization. Cell culture experiments with HUVECs demonstrated that smaller size HA (5 kDa and 60 kDa HA) stimulated cell spreading, migration and viability compared to high molecular weight HA. We expect that the knowledge obtained from these studies will take us a step closer to developing new HA-based biomaterials as potential therapeutic solutions for vascular diseases.

Conflicts of interest

There are no conflicts to declare.

Acknowledgements

Xinqing Pang acknowledges School of Engineering and Materials Science at Queen Mary University of London for her PhD scholarship. Weiqi Li thanks European Commission for his post-doctoral funding. Yichen Yuan thanks China Scholarship Council for her PhD Scholarship (No. 201706630005). The authors thank Dominic Collis and Clare O'Malley for useful discussions relating to this project.

References

1. J. R. E. Fraser, T. C. Laurent and U. B. G. Laurent, *Journal of Internal Medicine*, 1997, **242**, 27-33.
2. B. P. Toole, *Nat Rev Cancer*, 2004, **4**, 528-539.
3. B. V. Nusgens, *Ann Dermatol Venereol*, 2010, **137 Suppl 1**, S3-8.
4. R. O. Hynes, *Science*, 2009, **326**, 1216-1219.
5. Y. Zeng, M. Waters, A. Andrews, P. Honarmandi, E. E. Ebong, V. Rizzo and J. M. Tarbell, *AJP: Heart and Circulatory Physiology*, 2013, **305**, H811-H820.
6. R. Lindner and H. Y. Naim, *Experimental Cell Research*, 2009, **315**, 2871-2878.
7. C. C. Michel and F. E. Curry, *Physiological reviews*, 1999, **79**, 703-761.
8. J. R. Levick and C. C. Michel, *Cardiovasc Res*, 2010, **87**, 198-210.
9. J. M. Tarbell, *Cardiovasc Res*, 2010, **87**, 320-330.
10. H. Vink and B. R. Duling, *Circulation Research*, 1996, **79**, 581-589.
11. H. H. Lipowsky, *Annals of Biomedical Engineering*, 2012, **40**, 840-848.
12. T. Pavicic, G. G. Gauglitz, P. Lersch, K. Schwach-Abdellaoui, B. Malle, H. C. Korting and M. Farwick, *Journal of Drugs in Dermatology*, 2011, **10**, 990-1000.
13. E. Gatto and M. Venanzi, *Polymer Journal*, 2013, **45**, 468.
14. G. M. Whitesides, J. K. Kriebel and J. C. Love, *Science progress*, 2005, **88**, 17-48.
15. M. Mrksich and G. M. Whitesides, *Annual Review of Biophysics and Biomolecular Structure*, 1996, **25**, 55-78.
16. J. C. Love, L. A. Estroff, J. K. Kriebel, R. G. Nuzzo and G. M. Whitesides, *Chem Rev*, 2005, **105**, 1103-1169.
17. F. Schreiber, *Progress in Surface Science*, 2000, **65**, 151-256.
18. D. K. Schwartz, *Annual review of physical chemistry*, 2001, **52**, 107-137.
19. M. J. Pellerite, T. D. Dunbar, L. D. Boardman and E. J. Wood, *The Journal of Physical Chemistry B*, 2003, **107**, 11726-11736.

20. R. G. Nuzzo and D. L. Allara, *Journal of the American Chemical Society*, 1983, **105**, 4481-4483.
21. J. Christopher Love, D. B. Wolfe, R. Haasch, M. L. Chabinyc, K. E. Paul, G. M. Whitesides and R. G. Nuzzo, *Journal of the American Chemical Society*, 2003, **125**, 2597-2609.
22. C. D. Bain, E. B. Troughton, Y. T. Tao, J. Evall, G. M. Whitesides and R. G. Nuzzo, *Journal of the American Chemical Society*, 1989, **111**, 321-335.
23. R. H. Terrill, T. a. Tanzer and P. W. Bohn, *Langmuir*, 1998, **14**, 845-854.
24. N. Leventis and Y. C. Chung, *Journal of The Electrochemical Society*, 1991, **138**, L21-L21.
25. C. M. Whelan, M. R. Smyth, C. J. Barnes, N. M. D. Brown and C. a. Anderson, *Applied Surface Science*, 1998, **134**, 144-158.
26. F. Patolsky, M. Zayats, E. Katz and I. Willner, *Analytical Chemistry*, 1999, **71**, 3171-3180.
27. F. Höök, *PhD Thesis*, 1997.
28. S. H. Brewer, A. M. Allen, S. E. Lappig, T. L. Chasse, K. A. Briggman, C. B. German and S. Franzen, *Langmuir*, 2004, **20**, 5512-5520.
29. T. Wink, S. J. van Zuilen, A. Bult and W. P. van Bennekom, *The Analyst*, 1997, **122**, 43R-50R.
30. D. Nedelkov and R. W. Nelson, *Trends Biotechnol*, 2003, **21**, 301-305.
31. M. Balcells, D. Klee, M. Fabry and H. Höcker, *Journal of colloid and interface science*, 1999, **220**, 198-204.
32. A. K. Nowinski, F. Sun, A. D. White, A. J. Keefe and S. Jiang, *Journal of the American Chemical Society*, 2012, **134**, 6000-6005.
33. M. Mrksich, *Acta Biomaterialia*, 2009, **5**, 832-841.
34. M. E. Mummert, M. Mohamadzadeh, D. I. Mummert, N. Mizumoto and A. Takashima, *The Journal of experimental medicine*, 2000, **192**, 769-779.
35. Y. N. Xia and G. M. Whitesides, *Angew Chem Int Edit*, 1998, **37**, 550-575.
36. D. Qin, Y. N. Xia and G. M. Whitesides, *Nature Protocols*, 2010, **5**, 491-502.
37. D. H. Jiang, J. R. Liang, J. Fan, S. Yu, S. P. Chen, Y. Luo, G. D. Prestwich, M. M. Mascarenhas, H. G. Garg, D. A. Quinn, R. J. Homer, D. R. Goldstein, R. Bucala, P. J. Lee, R. Medzhitov and P. W. Noble, *Nature Medicine*, 2005, **11**, 1173-1179.
38. J. Gajewiak, S. S. Cai, X. Z. Shu and G. D. Prestwich, *Biomacromolecules*, 2006, **7**, 1781-1789.
39. D. S. Ferreira, A. P. Marques, R. L. Reis and H. S. Azevedo, *Biomaterials Science*, 2013, **1**, 952-964.
40. B. P. Orner, R. Derda, R. L. Lewis, J. A. Thomson and L. L. Kiessling, *Journal of the American Chemical Society*, 2004, **126**, 10808-10809.
41. R. Derda, S. Musah, B. P. Orner, J. R. Klim, L. Y. Li and L. L. Kiessling, *Journal of the American Chemical Society*, 2010, **132**, 1289-1295.
42. S. F. Chen, Z. Q. Cao and S. Y. Jiang, *Biomaterials*, 2009, **30**, 5892-5896.
43. R. McMillan, B. Meeks, F. Bensebaa, Y. Deslandes and H. Sheardown, *Journal of Biomedical Materials Research*, 2001, **54**, 272-283.
44. M. Boncheva and H. Vogel, *Biophysical Journal*, 1997, **73**, 1056-1072.
45. L. Y. Li, J. R. Klim, R. Derda, A. H. Courtney and L. L. Kiessling, *Proceedings of the National Academy of Sciences of the United States of America*, 2011, **108**, 11745-11750.
46. Y. Shi, R. Lin, H. Cui and H. S. Azevedo, *Methods Mol Biol*, 2018, **1758**, 11-26.
47. M. V. Voinova, M. Rodahl, M. Jonson and B. Kasemo, *Phys Scripta*, 1999, **59**, 391-396.
48. A. Francesko, D. S. da Costa, P. Lisboa, R. L. Reis, I. Pashkuleva and T. Tzanov, *Journal of Materials Chemistry*, 2012, **22**, 19438-19446.
49. D. G. Castner, K. Hinds and D. W. Grainger, *Langmuir*, 1996, **12**, 5083-5086.
50. C. Vericat, M. E. Vela, G. Benitez, P. Carro and R. C. Salvarezza, *Chemical Society Reviews*, 2010, **39**, 1805-1834.
51. W. Mo, C. Yang, Y. Liu, Y. He, Y. Wang and F. Gao, *Acta Biochim Biophys Sin (Shanghai)*, 2011, **43**, 930-939.
52. D. C. West and S. Kumar, *Exp Cell Res*, 1989, **183**, 179-196.
53. C. H. Antoni, Y. McDuffie, J. Bauer, J. P. Sleeman and H. Boehm, *Frontiers in Bioengineering and Biotechnology*, 2018, **6**, 1-7.
54. S. Ibrahim, B. Joddar, M. Craps and A. Ramamurthi, *Biomaterials*, 2007, **28**, 825-835.